

Carbon nanotube tipped atomic force microscopy for measurement of <100 nm etch morphology on semiconductors

G. Nagy, M. Levy, R. Scarmozzino, and R. M. Osgood, Jr.

Microelectronics Sciences Laboratories, Columbia University, New York, New York 10027

H. Dai^{a)} and R. E. Smalley

Center for Nanoscale Science and Technology, Rice University, Houston, Texas 77251

C. A. Michaels^{b)} and G. W. Flynn

Department of Chemistry, Columbia University, New York, New York 10027

G. F. McLane

U.S. Army Research Laboratory, Ft. Monmouth, New Jersey 07703

(Received 7 January 1998; accepted for publication 26 May 1998)

The use of carbon nanotubes as tips in atomic force microscopy for a systematic study of dry etching pattern transfer in GaAs is described. The GaAs samples are patterned via electron beam lithography and then etched using magnetron reactive ion or chemically assisted ion beam processing. The technique allows diagnosis, in air, of etched features with scale sizes of <100 nm.

© 1998 American Institute of Physics. [S0003-6951(98)04930-4]

While there has been a considerable volume of research directed at understanding the electronic^{1,2} and mechanical properties,^{3,4} and production mechanisms⁵⁻⁷ of carbon nanotubes,⁸ their technological applications have received far less attention. Recently, the advantages of carbon nanotubes as tips in atomic force microscopy have been described and demonstrated.⁹ Because of the small diameter (1–10 nm), high aspect ratio, and, in some cases, smooth end termination of nanotube tips, atomic force microscopy (AFM) with nanotube tips allows imaging of relatively deep features at near nanometer resolution. In addition, while conventional silicon tips may generate impact forces >100 nN on the surface, the maximum force transmitted by nanotube probes is limited by the Euler buckling force of <10 nN. After the Euler buckling force is exceeded, the carbon nanotube tips bend easily with little additional force, resulting in gentle imaging ability as well as tip longevity. Since the technique can be readily used in an air environment, it provides a complementary capability to scanning electron microscopy (SEM).

There is also considerable interest in the fabrication of ultrasmall (<100 nm) features in elemental and III–V semiconductors for their potential applications in electronic and photonic devices. The usefulness of these features depends on their morphological and electronic properties which, in turn, may be heavily dependent on the details of the pattern transfer process that is used to fabricate the structures.¹⁰⁻¹² An excellent example of the issues involved in the transfer process is the tradeoff between ion energy and chemical etching encountered in the dry etch process. Higher energy ions are necessary to provide sufficient etch anisotropy to give vertical sidewalls; purely chemical-based etching leads to undercutting of these sidewalls. However, if the ion energy is too high, the surface mask will be eroded yielding rounded or even severely eroded features. Although these

issues of etching morphology are relevant for all feature sizes, they become extremely difficult to control for features whose dimensions are in the nanometer regime. Furthermore, since the role of the surface becomes progressively more important as the feature size decreases, at nanometer-scale structures the electronic and optical properties of the feature can be dominated by sidewall effects such as surface recombination and near-surface damage.

The use of nanotube AFM as a probe of microfabricated components was first described by Dai *et al.*⁹ In this letter we present a study which shows the utility of this technique in observing and diagnosing the interplay of physical processes important in dry etching of features of <100 nm scale size. For this study, nanometer-scaled features are fabricated in GaAs-based materials using two different etching techniques, magnetron enhanced reactive ion etching (MIE)¹³ and chemically assisted ion beam etching (CAIBE).¹⁴⁻¹⁶ The morphology of the structures etched using MIE and CAIBE are investigated as a function of etching parameters using AFM with carbon nanotube tips, as well as SEM.

To evaluate the etching conditions necessary for the fabrication of ultrasmall structures, highly doped *n*-GaAs (100) substrates were used. The mask pattern was fabricated at the Cornell Nanofabrication Facility using electron-beam lithography on a 30 nm Ni thin film. The MIE etch experiments were conducted in a MRC 710 magnetron reactive ion etch system at the Army Research Laboratory at Ft. Monmouth using a chamber pressure of 2 mTorr and a BCl₃ flow rate of 2 sccm. Samples were etched at various combinations of rf power (correlating with sample bias) and etch time to investigate the effects of these parameters on feature morphology. The CAIBE experiments were performed using a 3 cm Kaufman source with 500 eV Ar ions at a pressure of 2×10^{-4} Torr and Cl₂ as the reactive gas at various flow rates. The surface etch depth and feature morphology were evaluated after each experiment using scanning electron microscopy or carbon nanotube tipped atomic force microscopy. The carbon nanotubes were attached to cobalt-coated silicon cantilevers, using the procedure outlined in Ref. 17.

^{a)}Present address: Department of Chemistry, Stanford University, Stanford, CA 94305.

^{b)}Present address: National Institute of Standards and Technology, Gaithersburg, MD 20899.

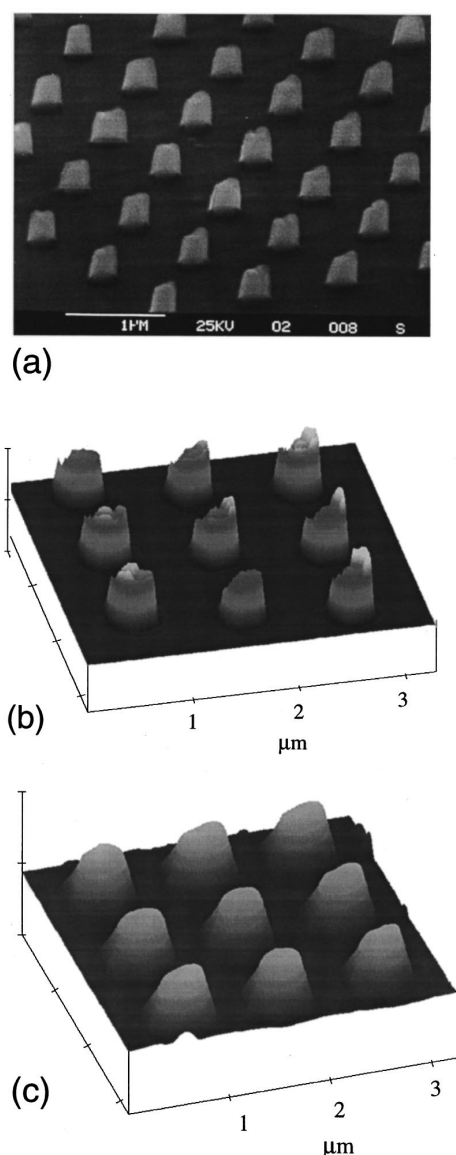


FIG. 1. Comparison of SEM (a), nanotube tipped AFM (b), and standard silicon nitride tipped AFM (c) images of etched features in GaAs. The structures were fabricated using CAIBE with a chlorine flow rate of 50 sccm and an ion beam current density of 1.1 mA/cm^2 .

Carbon nanotube tipped AFM imaging of nanostructures was first examined at relatively large scale, $\sim 200 \text{ nm}$, since the overall contour of features with this dimension can be imaged independently with a SEM. In addition, these same features were also examined with a standard silicon nitride tipped AFM in order to compare the highest spatial resolutions, i.e., those $\ll 200 \text{ nm}$, with those scanned with the nanotube tip. The silicon nitride tip used for this comparison was a Digital Instruments oxide-sharpened probe with a square pyramidal shape. The oxide sharpening process for this tip produces a cusp-shaped end (near the last 100–200 nm of the tip) with a nominal tip radius of curvature of $\leq 20 \text{ nm}$, for high resolution imaging. For this comparison, the features (Fig. 1) were etched via CAIBE using 200 nm diameter masks fabricated with electron beam lithography and liftoff of a 100 nm Cr/200 nm Au thin film on GaAs.

All three pictures of the etched features in Fig. 1 show the same overall surface morphology, resulting from a choice

of aggressive etching conditions. In particular, the features display slightly sloping sidewalls and cusped tops. Notice, however, that the nanotube AFM scan provides far more detailed information about the condition of the masks than either the SEM or the silicon nitride tipped AFM images. The nanotube picture shows clearly the uneven, craterlike appearance of the structures with surface spatial features as small as $\sim 30 \text{ nm}$ clearly discernable. The high resolution makes it possible to detect consistent details in the erosion pattern from feature to feature, involving an apparent enhanced erosion at the feature center and transverse nonuniformity from right to left in the scan. Not all the features on the etched sample were eroded in this manner and, probably as a result of nonuniform mask deposition, regions of relatively smoothly etched features were also evident. The sidewall slope of the structures is measured at 80° , well below the 88° resolution limit of this nanotube AFM scan; this limit was set by the AFM sampling interval in the horizontal direction and the height of the features. In comparison, the silicon nitride tip measured this slope at 73° . As a result of the size and geometry of the silicon nitride tip, the images obtained with it show features that are larger and have greater sidewall slopes than the actual features. Finally, the nanotube AFM image also reveals slight trenching at the base, a feature not evident in the other scans. Such trenching is known to occur as a result of the deflection of bombarding ions by the sidewalls during etching.

Examples of the utility of carbon nanotube tipped AFM in the diagnosis of this ion energy dependence of etch morphology are shown in Fig. 2 for MIE-etched features. Here, samples with 70 nm diameter circular mask patterns were etched with different sample biases and time durations, i.e., 400 W rf power for 10 s [Fig. 2(a)], and 20 s [Fig. 2(b)], and with 200 W for 20 s [Fig. 2(c)]. The 400 and 200 W input powers correspond to sample biases of 75 and 30 V, respectively. The AFM pictures show clearly the strong dependence of feature morphology on the etching parameters. For the sample etched with 400 W for 10 s, the features are anisotropically etched and have diameters of $\sim 75 \text{ nm}$. Note that the masks are pointed due to erosion of the mask edges; this same process has led to etch-induced sloping of the sidewalls. As a result, as shown in Fig. 2(b), a longer etch time with the same power caused the surface masks to be completely eroded and, consequently, the features were destroyed. At lower ion energies [Fig. 2(c)] the structures had larger average widths, $\sim 120 \text{ nm}$, because at these ion energies the etching was not as directionally well defined. However, the lower ion energies also caused the mask erosion to be not as pronounced as in Fig. 2(a), or even more clearly in Fig. 2(b), and hence all the features are intact.

These results may be compared with studies of MIE etching of somewhat larger diameter features. Luminescence studies of MIE-etched microsized features¹⁰ show lower sidewall damage at 400 W rf power than at 200 W. This is due to the higher directional character of the ion bombardment at higher bias. Interestingly, the etching of features at these larger diameters, also with an approximate unity aspect ratio, showed little or no degradation of the mask. Presumably this is simply a result of the larger feature size compared to the usual edge degradation. However, with the

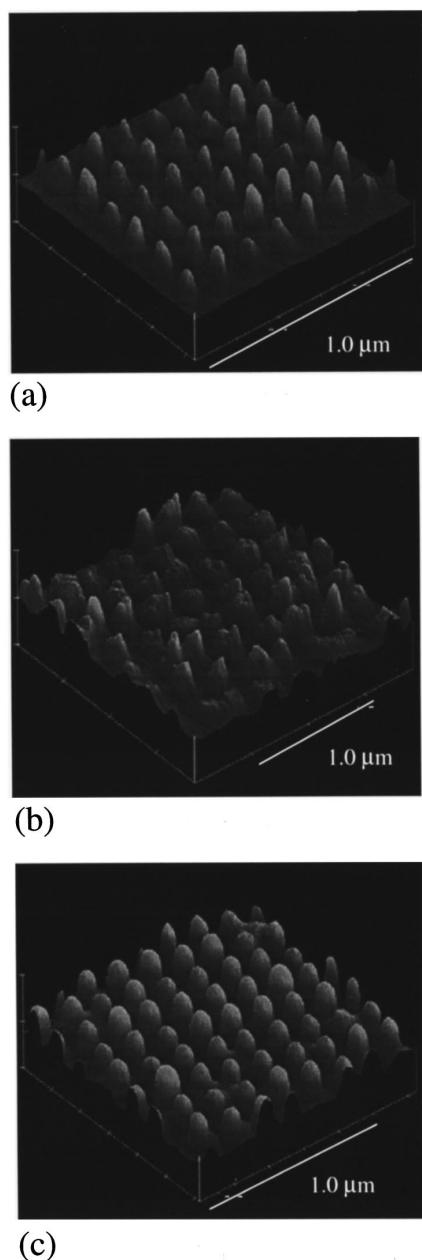


FIG. 2. Carbon nanotube tipped AFM pictures of features showing various degrees of mask deterioration after MIE etching. The rf power and etch durations were: (a) 400 W, 10 s; (b) 400 W, 20 s; (c) 200 W, 20 s.

smaller feature sizes fabricated here, higher power resulted in greater degradation of feature morphology.

The advantages of the small size of the carbon nanotube tips in the accurate imaging of small features can also be shown clearly by using recently developed deconvolution/convolution procedures developed for AFM tips. Several researchers have developed the mathematical modeling of image features obtained by assuming simple “hard-surface” geometrical interactions with finite tip dimensions.^{18–20} For example, the model of Keller presents an algorithm for deriving the true surface structure from known image and tip geometries, using transforms of the image, tip, and surface:²⁰

$$\begin{aligned} [\partial^2 s(\mathbf{x}) / \partial x_i \partial x_j]^{-1} = & [\partial^2 i(\mathbf{x}') / \partial x_i \partial x_j]^{-1} \\ & + [\partial^2 t(\Delta \mathbf{x}) / \partial \Delta x_i \partial \Delta x_j]^{-1}, \end{aligned} \quad (1)$$

where $s(\mathbf{x})$, $i(\mathbf{x}')$, and $t(\Delta \mathbf{x})$ are the profile functions of the

sample surface, the image, and the tip, respectively, in terms of the coordinates of the surface \mathbf{x} , and of the image \mathbf{x}' , with $\Delta \mathbf{x} = \mathbf{x} - \mathbf{x}'$. Such deconvolution algorithms may be readily used for tips with well characterized geometries.²⁰ A computer program developed for this purpose by Markiewicz *et al.*²¹ can be easily applied to standard or nanotube tips and also shows the utility of carbon nanotube tips for producing higher resolution images.

In summary, atomic force microscopy using carbon nanotube tips has been applied to diagnose the morphological characteristics of etched nanoscale GaAs features. GaAs structures with Cr/Au masks, fabricated via chemically assisted ion beam etching, were diagnosed utilizing carbon nanotube tipped AFM, which was able to detect small details of feature degradation not visible with standard silicon nitride tipped AFM or SEM. Atomic force microscopy with carbon nanotube tips was also applied to the evaluation of magnetron reactive ion etching in the fabrication of features in GaAs down to 70 nm in diameter. The nanotube AFM images showed with high resolution the extent of feature erosion under certain etch conditions.

Finally, G.N., M.L., R.S., and R.M.O. wish to acknowledge partial support of this work by AFOSR/ARPA under Contract No. F49620-92-J-0414 and by JSEP under Contract No. DAAG55-97-1-0166. H.D. and R.E.S. would like to acknowledge support from NSF Contract No. DMR-9522251. C.A.M. and G.W.F. wish to acknowledge support from NSF Contract No. DMR-9424296. The authors would also like to thank Leanna Giancarlo for help with AFM imaging.

¹J. W. Mintmire, B. I. Dunlap, and C. T. White, *Phys. Rev. Lett.* **68**, 631 (1992).

²M. Kosaka, T. W. Ebbesen, H. Hiura, and K. Tanigaki, *Chem. Phys. Lett.* **233**, 47 (1995).

³J. F. Despres, E. Daguerre, and K. Lafdi, *Carbon* **33**, 87 (1995).

⁴M. M. J. Treacy, T. W. Ebbesen, and J. M. Gibson, *Nature (London)* **381**, 678 (1996).

⁵T. W. Ebbesen, *Annu. Rev. Mater. Sci.* **24**, 235 (1994).

⁶M. Ge and K. Sattler, *Science* **260**, 515 (1993).

⁷N. Hatta and K. Murata, *Chem. Phys. Lett.* **217**, 398 (1994).

⁸*Carbon Nanotubes-Preparation and Properties*, edited by T. W. Ebbesen (CRC, Boca Raton, 1997).

⁹H. Dai, J. H. Hafner, A. G. Rinzler, D. T. Colbert, and R. E. Smalley, *Nature (London)* **387**, 147 (1996).

¹⁰M. Freiler, G. F. McLane, S. Kim, M. Levy, R. Scarmozzino, I. P. Herman, and R. M. Osgood, Jr., *Appl. Phys. Lett.* **67**, 1 (1995).

¹¹A. Scherer, H. G. Craighead, M. L. Roukes, and J. P. Harbison, *J. Vac. Sci. Technol. B* **6**, 277 (1988).

¹²J. W. Coburn, *Appl. Phys. A: Solids Surf.* **59**, 451 (1994).

¹³G. F. McLane, M. Mayyappan, M. W. Cole, and C. Wrenn, *J. Appl. Phys.* **69**, 695 (1991).

¹⁴M. W. Geis, G. A. Lincoln, N. Efremow, and W. J. Piacentini, *J. Vac. Sci. Technol.* **19**, 1390 (1981).

¹⁵J. D. Chinn, A. Fernandez, I. Adesida, and E. D. Wolf, *J. Vac. Sci. Technol. A* **1**, 701 (1983).

¹⁶Y. S. Chieh, J. P. Krusius, and P. Chapman, *J. Electrochem. Soc.* **141**, 1585 (1994).

¹⁷J. H. Hafner, Nanotube Tips for SFM, on the Internet at <http://www.cnst.rice.edu/mount.html>

¹⁸P. Markiewicz and C. Goh, *J. Vac. Sci. Technol. B* **13**, 1115 (1995).

¹⁹D. L. Wilson, K. S. Kump, S. J. Eppell, and R. E. Marchant, *Langmuir* **11**, 265 (1995).

²⁰D. Keller, *Surf. Sci.* **253**, 353 (1991).

²¹P. Markiewicz, *Deconvolution of AFM Images*, on the Internet at <http://www.chem.utoronto.ca/~pmarkiew/>.